arXiv:1412.7079v2 [cond-mat.str-el] 24 Dec 2014

Interplay between tetragonal magnetic order, stripe magnetism, and superconductivity in iron-based materials

Jian Kang, Xiaoyu Wang, Andrey V. Chubukov, and Rafael M. Fernandes

School of Physics and Astronomy, University of Minnesota, Minneapolis, MN 55455, USA

Motivated by recent experiments in $Ba_{1-x}K_xFe_2As_2$ [A. E. Böhmer *et al*, to be published], we analyze the type of spin-density wave (SDW) order in doped iron-pnictides and the discontinuities of the superconducting transition temperature T_c in the coexistence phase with SDW magnetism. By tracking the magnetic transition line $T_N(x)$ towards optimal doping within an itinerant fermionic model, we find a sequence of transitions from the stripe-orthorhombic (C_2) SDW order to the tetragonal (C_4) order and then back to the C_2 order. We argue that the superconducting T_c has two discontinuities – it jumps to a smaller value upon entering the coexistence region with the C_4 magnetic phase, and then jumps to a larger value inside the SDW state when it crosses the boundary between the C_4 and C_2 SDW orders. The full agreement with the experimental phase diagram provides a strong indication that the itinerant approach is adequate to describe the physics of weakly/moderately doped iron-pnictides.

Introduction. One of the key features of the iron-based superconductors is the proximity or coexistence of superconductivity with a spin-density wave (SDW) magnetic order [1]. The stripe-type magnetic order (spins aligned ferromagnetically in one direction and antiferromagnetically in the other) has been observed experimentally in numerous undoped and weakly doped materials below $T_N \sim 150K$ [2, 6]. Such an order breaks the $O(3)$ spin-rotational symmetry and also breaks the tetragonal (C_4) lattice rotational symmetry down to orthorhombic (C_2). Theoretically, the stripe order has been found in both itinerant [3–5, 7–9] and localized spin [10–12] approaches to Fe-pnictides. In the itinerant scenario, stripe order originates from the interaction between fermions near hole and electron pockets, which are separated by $\mathbf{Q}_1 = (0, \pi)$ and $\mathbf{Q}_2 = (\pi, 0)$ in the Fe-only Brillouin zone. Fluctuations of the stripe order above the magnetic ordering temperature T_N were further argued [4, 13] to split the $O(3)$ and C_4 transitions and give rise to the observed nematic-type order at $T_N < T < T_{\rm nem}$ in which the C_4 lattice rotational symmetry is broken down to C_2 but the $O(3)$ spin-rotational symmetry remains unbroken.

A recent experiment on the hole-doped 122 Fe-pnictide $Ba_{1-x}K_xFe_2As_2$ (Ref. [19]), however, found that the stripe magnetic configuration does not persist at all dopings where magnetic order has been observed. Instead, in some doping range, the stripe magnetic phase is replaced by another SDW state in which the tetragonal C_4 symmetry is unbroken. Neutron scattering experiments in the related compound $Ba_{1-x}Na_xFe_2As_2$ (Ref. [18]) reported a similar C_4 SDW phase, with the spin response still peaked at $\mathbf{Q}_1$ and $\mathbf{Q}_2$. The most natural explanation for such a C_4 SDW phase is a magnetic configuration with equal magnetic spectral weight at the $\mathbf{Q}_1$ and $\mathbf{Q}_2$ ordering vectors, resulting either in a orthogonal checkerboard or in a non-uniform spin pattern (see Refs. [3, 8, 11, 22–25]). Hereafter we label this phase as C_4 SDW order and the stripe phase as C_2 SDW order. Both C_4 and C_2 SDW orders were found experimentally [18, 19] to coexist with superconducting (SC) order. The detailed analysis of the boundaries of the C_4 SDW phase in the phase diagram of $Ba_{1-x}K_xFe_2As_2$ (Ref. [19]) shows several prominent features that require theoretical explanation (see Fig. 1): (i) The C_4 SDW phase is confined to a narrow doping range with relatively low T_N values, being sandwiched by two regions with C_2 SDW order at lower and higher doping levels. (ii) The C_4 SDW phase is confined to the near-vicinity of the magnetic instability line T_N and does not extend deep into the magnetically ordered region. (iii) The superconducting T_c is discontinuous at the onset of the coexistence with C_4 SDW, where it jumps *down* by a finite amount. (iv) T_c is again discontinuous when it crosses the boundary between C_4 and C_2 SDW orders inside the SC coexistence region, jumping *up* by a finite amount.

In this communication we argue that all four features can be naturally explained within the itinerant scenario for magnetism in iron-pnictides. We depart from a model of interacting electrons located near hole and electron pockets and derive and analyze the Ginzburg-Landau (GL) free-energy for the coupled SDW and SC order parameters. We first analyze the structure of the SDW order alone. We argue, based on the analysis of GL expansion to fourth order, that the parameter that determines whether the SDW order is C_2 or C_4 immediately below T_N changes sign twice along the $T_N(x)$ line. For large and small values of T_N the stripe order wins, whereas for intermediate T_N values the C_4 SDW order wins, explaining observation (i) above. We then extend the GL analysis into the ordered phase by expanding it to higher (sixth) order, showing that larger values of the magnetic order parameter favor the stripe C_2 phase, even if the initial instability is towards the C_4 SDW order. This restricts the C_4 phase to the vicinity of the T_N instability line, explaining the experimental feature (ii).

We then analyze the GL model for interacting SDW and s^{+-} SC order parameters. We first argue that the jump of T_c to a smaller value at the onset of coexistence

with SDW is a natural consequence of the experimental fact that the SC transition line T_c crosses T_N at doping levels where the magnetic transition is first-order. Specifically, the sign of the biquadratic coupling between the s^{+-} SC and SDW order parameters [14, 15] is such that the jump in the SDW order parameter at the point where the T_N and T_c lines meet causes a jump of T_c to a smaller value, consistent with observation (iii). We then analyze the behavior of T_c inside the SDW+SC coexistence state, as it crosses the boundary between the C_4 and C_2 SDW phases. We argue that T_c again jumps, this time to a larger value. The discontinuity is due to the fact that the energy of the $C_2+\mathrm{SC}$ phase is lower than that of the $C_4+\mathrm{SC}$ phase by a finite amount because in the $C_2+\mathrm{SC}$ phase the system necessarily develops a d-wave component of the SC order parameter due to the breaking of the C_4 symmetry [17]. We show that this gives rise to an additional gain of condensation energy, resulting in a higher T_c in the $C_2+\mathrm{SC}$ phase compared to T_c in the $C_4+\mathrm{SC}$ phase. This is consistent with the experimental observation (iv). This last effect is additionally enhanced in $Ba_{1-x}K_xFe_2As_2$ because the sub-leading d-wave instability is nearly degenerate with the leading s^{+-} instability [26, 29, 33–35], as seen for instance by recent Raman experiments [27, 28].

We interpret the good agreement between our itinerant theory and the experimental data, including fine details, as a strong indication that the itinerant approach to magnetism in Fe-pnictides is capable to explain the physics of these materials. The situation may be different in 11 Fe-chalcogenides where, at least for the parent FeTe, magnetic order involves different momenta and cannot be naturally obtained within an itinerant scenario [5, 6, 20, 36].

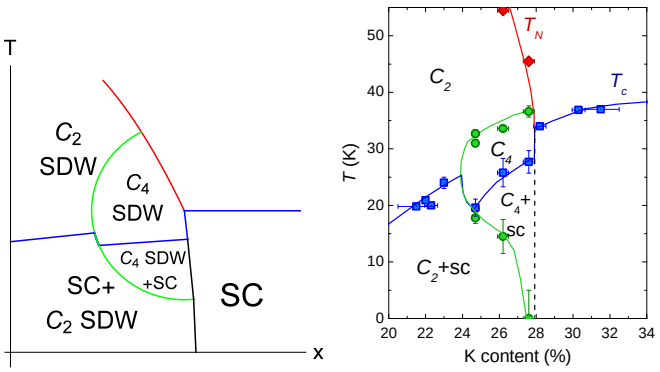

FIG. 1: Schematic phase diagram resulting from our itinerant model (left) and experimental phase diagram of Ref. [19] for $Ba_{1-x}K_xFe_2As_2$ (right). Blue lines refer to the (second-order) SC phase transition whereas the green and red lines refer to the (first-order) C_4-C_2 and normal state-SDW phase transitions, respectively. Black lines refer to the first order SDW phase transitions inside SC phase. The four experimental features discussed in the main text (i)-(iv) are naturally captured by the itinerant model. The precise shapes of the transition lines is non-universal and depends on details of the model not included here.

The model. We consider the three-band 2D model with one circular hole pocket centered at $(0,0)$ and two elliptical electron pockets centered at $(\pi,0)$ and $(0,\pi)$ in the Fe-only Brillouin zone. This is the minimal model to account for itinerant $\mathbf{Q}_1/\mathbf{Q}_2$ magnetism [3, 4, 14, 15]. The inclusion of other two hole pockets complicates calculations but does not lead to new physics. We follow previous works [3, 4] and approximate the band dispersions as parabolic ones, $H_0=\sum_{\boldsymbol{k}a\alpha}\epsilon_{\boldsymbol{k}a}c^\dagger_{\boldsymbol{k}a\alpha}c_{\boldsymbol{k}a\alpha}$, with:

$$\begin{aligned}\epsilon_{\boldsymbol{k}h}&=-\epsilon_{\boldsymbol{k}}=\frac{k^2}{2m}-\epsilon_0\\ \epsilon_{e_{1/2},\boldsymbol{k}+\boldsymbol{Q}_{1/2}}&=\epsilon_{\boldsymbol{k}}+(\delta_\mu\pm\delta_m\cos 2\theta)\end{aligned}\tag{1}$$

where $\boldsymbol{k}$, a, and α refer to the momentum, band, and spin indices, respectively. δ_μ measures the chemical doping, δ_m accounts for the ellipticity of the electron pockets, and θ is the angle around an elliptical electron pocket. The two interactions relevant to SDW order are density-density (U_1) and pair-hopping (U_3) interactions between hole and electron pockets (see Refs. [3, 4]). They act identically in the SDW channel and drive the system towards the SDW state with ordering vectors $\boldsymbol{Q}_1/\boldsymbol{Q}_2$, which are the momentum displacements between the centers of electron and hole pockets. To obtain the GL free-energy we introduce two SDW fields $\boldsymbol{M}_i(\boldsymbol{q})=(U_1+U_3)\sum_k c^\dagger_{\boldsymbol{k}+\boldsymbol{q},h}\frac{\boldsymbol{\sigma}}{2}c_{\boldsymbol{k}+\boldsymbol{Q}_i,e_i}$, apply a Hubbard-Stratonovich transformation to decouple the 4-fermion interaction, integrate out the fermions, and expand the free-energy in powers of the SDW fields. To sixth order in $\boldsymbol{M}_i$, the free energy is expressed as

$$\begin{aligned}F(\boldsymbol{M}_i)=&\frac{a}{2}\left(\boldsymbol{M}_1^2+\boldsymbol{M}_2^2\right)+\frac{u}{4}\left(\boldsymbol{M}_1^2+\boldsymbol{M}_2^2\right)^2\\&-\frac{g}{4}\left(\boldsymbol{M}_1^2-\boldsymbol{M}_2^2\right)^2+w\left(\boldsymbol{M}_1\cdot\boldsymbol{M}_2\right)^2\\&-\frac{v}{6}\left(\boldsymbol{M}_1^2-\boldsymbol{M}_2^2\right)^2\left(\boldsymbol{M}_1^2+\boldsymbol{M}_2^2\right)\\&+\frac{\gamma}{6}\left(\boldsymbol{M}_1^2+\boldsymbol{M}_2^2\right)^3+\tilde{F}(\boldsymbol{M}_i)\end{aligned}\tag{2}$$

where $\tilde{F}(\boldsymbol{M}_i)$ stands for the terms with spatial and time derivatives. Note that the free-energy itself is invariant under C_4 rotations. All coefficients in Eq. (2) are the convolutions of fermionic Green's functions (two for a, four for u, g and w, and six for v and γ), and are expressed in terms of the band parameters from Eq. 1. We present the explicit results for these coefficients in the Supplementary Information (SI). All coefficients except for w, which vanishes in our model, are non-zero and depend on doping, temperature, and degree of ellipticity of the electron pockets.

C_2 vs C_4 magnetism. In the mean-field approximation, one neglects $\tilde{F}(\boldsymbol{M}_i)$ and obtains the equilibrium values of $\mathbf{M}_1$ and $\mathbf{M}_2$ by minimizing the free-energy. Let us first assume that $\mathbf{M}_{1,2}$ are small and restrict the analysis up to the quartic terms – i.e. we approach the transition from the paramagnetic side and check what happens immediately below T_N. One then finds in a straightforward way that the system develops C_2 order when $g>0$

and C_4 order when $g < 0$. For C_2 order, either $\boldsymbol{M}_1$ or $\boldsymbol{M}_2$ vanishes, whereas for C_4 order, $\boldsymbol{M}_1^2 = \boldsymbol{M}_2^2$. For $g > 0$, fluctuations contained in $\tilde{F}(\boldsymbol{M}_i)$ give rise to an intermediate nematic phase in which the C_4 symmetry is broken to C_2, but $\langle \boldsymbol{M}_i \rangle = 0$.

In Fig. 2 we show the behavior of g as a function of δ_μ/T_N, where the chemical potential δ_μ is proportional to doping. For simplicity we show a plot for fixed δ_m/T_N, but the behavior described here is generic (see SI). In the limit of high transition temperatures T_N (small doping), we find that $g \approx \frac{31\zeta(5)N_f\delta_m^2}{64\pi^4 T_N^4} > 0$, whereas as $T_N \to 0$ (optimal doping), $g \approx \frac{\delta_m^2 N_f}{|\delta_\mu|(\delta_\mu^2-\delta_m^2)^{3/2}} > 0$. For this last result, we used the fact that $|\delta_\mu| > \delta_m$ when $T_N \to 0$ [14]. Thus, in the high and low T_N regimes, the system develops a stripe C_2 order below $T_N(x)$. However, at intermediate T_N we find that g necessarily changes sign and becomes negative over some range of doping concetrations. Once $g < 0$, the system develops C_4 order. This explains the experimental observation (i) in $Ba_{1-x}K_xFe_2As_2$, i.e. that the doping range with C_4 order is sandwiched between two doping regions with C_2 order. Note that since g remains very small after it changes sign for the second time, the energies of both the C_4 and the C_2 SDW states are very close [18].

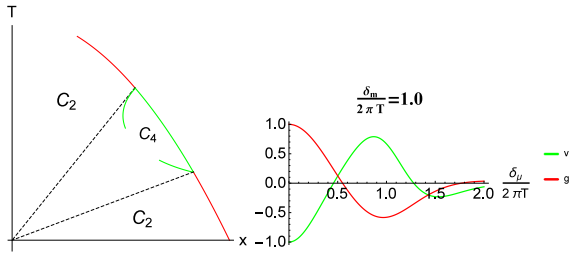

(a) (b)

FIG. 2: (a) The schematic phase diagram when SC is not included. The dashed (solid) lines give the phase boundary of C_4 SDW order in the absence (presence) of higher-order terms in the free energy. (b) The coefficients g and v in Eq. (2) (normalized to their $\delta_\mu = 0$ values) as functions of $\delta_\mu/(2\pi T)$ for $\delta_m/(2\pi T) = 1$. Note that g and v change sign twice as $\delta_\mu/(2\pi T)$ becomes larger. This behavior is generic for other values of $\delta_m/(2\pi T)$ (see the SI).

We next analyze how the boundaries of the C_4 order evolve as the system moves into the SDW phase. If we would restrict our analysis to the fourth-order terms in the free energy, the C_4 phase would extend all the way down to $T = 0$ (dashed lines in Fig. 2a). However, once the SDW order develops, higher-order terms in the GL free energy become relevant. In particular, the sixth-order term relevant for the $C_4 - C_2$ transition in Eq. (2) is $-\frac{v}{6}\left(\boldsymbol{M}_1^2 - \boldsymbol{M}_2^2\right)^2\left(\boldsymbol{M}_1^2 + \boldsymbol{M}_2^2\right)$. This term has the same $\left(\boldsymbol{M}_1^2 - \boldsymbol{M}_2^2\right)^2$ structure as the fourth order term $-\frac{g}{4}\left(\boldsymbol{M}_1^2 - \boldsymbol{M}_2^2\right)^2$ but scales additionally with the magnitude of $\mathbf{M}^2$. Combining the sixth-order and the fourth-order terms we find that the location of the boundaries between the C_4 and C_2 phases inside the SDW-ordered region is determined by the zeros of

$$\tilde{g} = g + \frac{2}{3}v\left(\boldsymbol{M}_1^2 + \boldsymbol{M}_2^2\right) \ , \tag{3}$$

The analytic expression for the coefficient v is presented in the SI. v can by itself be positive or negative, depending on doping. We show how the sign of v changes as function of δ_μ in Fig. 2. We note that in most of the region where $g < 0$, the coefficient v is positive, hence the sixth-order term prefers the C_2 phase and progressively shrinks the temperature range with C_4 order as the SDW order grows, resulting in the boundaries of the C_4 phase shown by the solid lines in Fig. 2a .We see this behavior as a strong indication that the C_4 phase progressively yields to the C_2 phase as SDW order grows, in agreement with the experimental determination of the C_4 line in $Ba_{1-x}K_xFe_2As_2$ (feature (ii) discussed in the Introduction).

The interplay between SDW and superconductivity. We now consider how the existence of both C_2 and C_4 phases affects the behavior of T_c in the state where SC and SDW coexist microscopically [31, 32]. We assume, as many authors before us, that superconductivity outside the coexistence region with SDW is of s^{+-} type, i.e. the SC order parameter is $s-$wave, but changes sign between hole and electron pockets [16]. We also assume that the SC transition in the absence of SDW is second order. Two inputs are needed to proceed our analysis: the character of the SDW transition and the location of the crossing point between the $T_c(x)$ and $T_N(x)$ transition lines.

The $C_2 - C_4$ transition is obviously first-order since in the C_2 phase one of the magnetic order parameters $\mathbf{M}_{1,2}$ is zero while in the C_4 phase both have equal magnitude. The character of the transition from the paramagnetic to the C_4 (or C_2) phase is determined by the interplay between the u and the γ terms in the GL free energy of Eq. (2) (Refs. [4, 14]). We found (see SI) that at least in the portion of the phase diagram where g is negative, u is also negative and γ is positive, implying that the transition into the C_4 SDW phase is first-order [21]. This is consistent with the experimental results [19], which found a weak first-order transition from the paramagnetic to the C_4 phase.

As for the location of the crossing point between the $T_c(x)$ and $T_N(x)$ lines, it can in principle be in the range where SDW order is either C_2 or C_4, depending on several input parameters of the model. In the experiments of Ref. [19], the crossing point happens in the range of C_4 order. We use this experimental result as an input and show that, in this situation, there must be two discontinuities in $T_c(x)$ in the region of coexistence with SDW order, consistent with the experimental findings (iii) and (iv) discussed in the Introduction.

Discontinuity of T_c at the onset of coexistence with SDW. We first consider how T_c evolves once the SC

transition line crosses the line of the first-order SDW transition into the C_4 phase. To achieve this, we write the GL model for coupled SDW and s^{+-} SC order parameters as [14, 15, 30]

$$\begin{aligned} F =& \frac{a}{2}\boldsymbol{M}^2 + \frac{u}{4}\boldsymbol{M}^4 + \frac{\gamma}{6}\boldsymbol{M}^6 + \frac{\alpha_s}{2}\left|\Delta_{s\pm}\right|^2 \\ &+ c\left|\Delta_{s\pm}\right|^2 \boldsymbol{M}^2 + \frac{\beta_s}{4}\left|\Delta_{s\pm}\right|^4 \ . \end{aligned} \tag{4}$$

where $\alpha_s = a_s(T - T_c)$ ($a_s > 0$) and $M^2 = \mathbf{M}_1^2 + \mathbf{M}_2^2 = 2\mathbf{M}_1^2$. As explained above, we have $u < 0$ and $\gamma > 0$, in which case the SDW transition into the C_4 phase is first-order. It occurs at $a = \frac{3u^2}{16\gamma}$, and M^2 jumps from zero to $M_0^2 = -\frac{3u}{4\gamma}$. An elementary analysis shows that a jump of M^2 at the SDW transition gives rise to a discontinuity in T_c as α_s is renormalized to $\tilde{\alpha}_s = \alpha_s + 2cM_0^2$. Hence

$$\delta T_c = \frac{3c}{2}\frac{u}{\gamma a_s} \ . \tag{5}$$

The remaining issue is whether δT_c is positive or negative. Because $u < 0$ and $\gamma > 0$, $\mathrm{sign}\,(\delta T_c) = -\mathrm{sign}\,(c)$. We computed the coefficient c in terms of parameters of the underlying fermionic model and found that c is *positive* (the details of the computations are presented in SI). Therefore, δT_c is negative, implying that the superconducting transition temperature jumps down upon entering the coexistence phase with SDW (see Fig. 1). A negative jump δT_c is consistent with the experimental observation (iii) outlined in the Introduction.

Discontinuity of T_c at the boundary between the C_2 and the C_4 phases. Finally, the experiment reveals that T_c is again discontinuous inside the SDW phase [19], when the SDW order switches from C_4 back to C_2 as doping decreases. Although the C_2-C_4 transition is first order, the coupling between $\left|\Delta_{s\pm}\right|^2$ and $\boldsymbol{M}^2$ cannot explain this discontinuity because $\boldsymbol{M}^2 = \boldsymbol{M}_1^2 + \boldsymbol{M}_2^2$ is continuous across the C_2-C_4 SDW phase transition. A more careful analysis, however, reveals that the c term in the free energy (4) arises from the combination of three distinct microscopic couplings between the magnetic order parameters and the gap functions at the hole pocket h and the electron pockets e_1 and e_2: $c_{hh}\left|\Delta_h\right|^2 \sum_i \boldsymbol{M}_i^2$, $c_{ee}\sum_i \boldsymbol{M}_i^2 \left|\Delta_{e_i}\right|^2$, and $c_{he}\sum_i \boldsymbol{M}_i^2\left(\Delta_h\Delta_{e_i}^* + \Delta_{e_i}\Delta_h^*\right)$. By symmetry, these three superconducting gaps can be equivalently recast in terms of an s^{++}, an s^{+-}, and a d-wave gap, as explained in the SI. Neglecting the s^{++} component, which does not distinguish between the C_4 and C_2 phases, we write the free-energy as

$$\begin{aligned} F =& \frac{a}{2}\boldsymbol{M}^2 + \frac{u}{4}\boldsymbol{M}^4 + \frac{\gamma}{6}\boldsymbol{M}^6 + \frac{\alpha_s}{2}\left|\Delta_{s\pm}\right|^2 + \frac{\alpha_d}{2}\left|\Delta_d\right|^2 \\ &+ c_s\left|\Delta_{s\pm}\right|^2 \boldsymbol{M}^2 + c_d\left|\Delta_d\right|^2 \boldsymbol{M}^2 \\ &+ c_{sd}\left(\Delta_{s\pm}^*\Delta_d + \text{h.c.}\right)\left(\boldsymbol{M}_1^2 - \boldsymbol{M}_2^2\right) + ... \ , \end{aligned} \tag{6}$$

The last term shows that the simultaneous presence of s^{+-} superconductivity and C_2 SDW order generates a d-wave component of the SC order parameter [17], even though the leading instability is not towards a d-wave SC phase – i.e. $\alpha_d = a_d(T - T_d) \approx a_d(T_c - T_d) > 0$ in Eq. (6). In more general terms, once the C_4 symmetry is broken down to C_2, the $s-$wave and $d-$wave SC order parameters no longer belong to different irreducible representations of the point group symmetry and the presence of one causes the appearance of the other.

We can now analyze the behavior of T_c in the coexistence phase with SDW. If the SDW is the C_4 phase, where $\boldsymbol{M}_1^2 = \boldsymbol{M}_2^2$, the last term in Eq. (6) is irrelevant, and the SC transition temperature is determined by $\tilde{\alpha}_s = \alpha_s + 2c_s\boldsymbol{M}^2 = 0$, i.e.

$$T_c^{(C_4)} = T_c - \frac{2c_s}{a_s}\boldsymbol{M}^2$$

If the SDW is the C_2 phase, the quadratic part of the SC GL free energy is given by:

$$F_{\text{SC}} = \frac{1}{2}\begin{pmatrix} \Delta_{s\pm} \\ \Delta_d \end{pmatrix}^T \begin{pmatrix} \tilde{\alpha}_s & 2c_{sd}\varphi \\ 2c_{sd}\varphi & \tilde{\alpha}_d \end{pmatrix} \begin{pmatrix} \Delta_{s\pm} \\ \Delta_d \end{pmatrix} \ , \tag{7}$$

where $\tilde{\alpha}_s = \alpha_s + 2c_s\boldsymbol{M}^2$, $\tilde{\alpha}_d = \alpha_d + 2c_d\boldsymbol{M}^2$, and $\varphi = \boldsymbol{M}_1^2 - \boldsymbol{M}_2^2$. Diagonalizing the matrix, we find that the superconducting T_c in the C_2 phase is given by $\tilde{\alpha}_s\tilde{\alpha}_d = (2c_{cd}\varphi)^2$, hence

$$T_c^{(C_2)} = T_c^{(C_4)} + \frac{4c_{cs}^2\varphi^2}{a_s a_d\left(T_c - T_d\right)} \tag{8}$$

The key point here is that even though $\boldsymbol{M}^2$ changes continuously across the $C_4 \to C_2$ transition, the quantity $\varphi = \boldsymbol{M}_1^2 - \boldsymbol{M}_2^2$ jumps from $\varphi = 0$ in the C_4 phase to $\varphi = \pm\boldsymbol{M}^2$ in the C_2 phase. As a result, T_c jumps *up* once the system moves from C_4 to C_2 SDW order inside the SDW-SC coexistence state. This is consistent with the experimental result (iv) discussed in the Introduction [19]. Note that the near degeneracy between the s^{+-} and the d-wave states, as attested by Raman scattering experiments [27, 28] in optimally doped $Ba_{1-x}K_xFe_2As_2$ implies that the T_c and T_d values are close, causing a visible jump in T_c.

Conclusions. In this communication we analyzed the structure of the SDW order arising from an itinerant fermionic model in doped iron-pnictides and its impact on the superconducting T_c in the coexistence phase with magnetism. We found that stripe magnetic order does not occur at all doping/temperatures where a magnetic instability is present – in particular, there is a narrow doping/temperature range located near the magnetic transition line $T_N(x)$ where the SDW order preserves the C_4 lattice rotational symmetry. We argued that, as the SC transition line crosses the SDW transition line, the superconducting T_c has two discontinuities – it jumps to a smaller value upon entering the coexistence region with C_4 SDW, and it jumps to a larger value inside the SDW state, when it crosses the boundary between C_4 and C_2 SDW orders. The resulting phase diagram, schematically shown in Fig. 1, is almost identical to the experimental phase diagram of the K-doped 122 material [19].

We view the agreement between theory and experiment, even in their fine details, as a strong indication that the itinerant approach is adequate to describe the physics of weakly/moderately doped Fe-pnictides.

We thank A. E. Böhmer, F. Hardy, and C. Meingast, for useful discussions and for sharing their data with us prior to publication. This work was supported by the Office of Basic Energy Sciences U. S. Department of Energy under awards numbers de-sc0012336 (XW, JK, and RMF) and DE-FG02-ER46900 (AVC).

[1] D. C. Johnston, Adv. Phys., **59**, 803 (2010); D.N. Basov and A.V. Chubukov, Nature Physics **7**, 241 (2011); J. Paglione and R. L. Greene, Nature Phys. **6**, 645 (2010); P. C. Canfield and S. L. Bud'ko, Annu. Rev. Cond. Mat. Phys. **1**, 27 (2010); H. H. Wen and S. Li, Annu. Rev. Cond. Mat. Phys. **2**, 121 (2011).

[2] see D. S. Inosov *et al.,* Nature Physics **6**, 178-181 (2010) and references therein.

[3] I. Eremin and A. V. Chubukov, Phys. Rev. B **81**, 024511 (2010).

[4] R. M. Fernandes, A. V. Chubukov, J. Knolle, I. Eremin and J. Schmalian, Phys. Rev. B **85**, 024534 (2012).

[5] M. D. Johannes and I. I. Mazin, Phys. Rev. B **79**, 220510 (2009).

[6] P. Dai, J. Hu, and E. Dagotto, Nature Phys. **8**, 709 (2012).

[7] V. Cvetkovic and Z. Tesanovic, Phys. Rev. B **80**, 024512 (2009).

[8] P. M. R. Brydon and C. Timm, Phys. Rev. B **79**, 180504(R) (2009); P. M. R. Brydon, J. Schmiedt, and C. Timm, Phys. Rev. B **84**, 214510 (2011).

[9] V. Cvetkovic and O. Vafek, Phys. Rev. B 88, 134510 (2013).

[10] C. Xu, M. Mueller, and S. Sachdev, Phys. Rev. B 78, 020501(R) (2008); C. Fang, H. Yao, W.-F. Tsai, J.P. Hu, and S. A. Kivelson, Phys. Rev. B 77 224509 (2008); E. Abrahams and Q. Si, J. Phys.: Condens. Matter 23, 223201 (2011).

[11] J. Lorenzana, G. Seibold, C. Ortix, and M. Grilli, Phys. Rev. Lett. **101**, 186402 (2008).

[12] Y. Kamiya, N. Kawashima, and C. D. Batista, Phys. Rev. B **84**, 214429 (2011).

[13] R. M. Fernandes, A. V. Chubukov, and J. Schmalian, Nature Phys. **10**, 97 (2014).

[14] A. B. Vorontsov, M. G. Vavilov, and A. V. Chubukov, Phys. Rev. B **79**, 060508 (2009)*; ibid* Phys. Rev. B **81**, 174538 (2010); M. G. Vavilov, A. V. Chubukov, A. B. Vorontsov, Supercond. Sci. Technol. **23**, 054011 (2010).

[15] R. M. Fernandes and J. Schmalian, Phys. Rev. B **82**, 014521 (2010).

[16] A. V. Chubukov, Annu. Rev. Cond. Mat. Phys. **3**, 57 (2012); P. J. Hirschfeld, M. M. Korshunov, and I. I. Mazin, Rep. Prog. Phys. **74**, 124508 (2011); K. Kuroki, H. Usui, S. Onari, R. Arita, and H. Aoki, Phys. Rev. B 79, 224511 (2009).

[17] R. M. Fernandes and A. J. Millis, Phys. Rev. Lett. **111**, 127001 (2013).

[18] S. Avci *et al.*, Nature Comm. **5**, 3845 (2014).

[19] A. E. Böhmer, F. Hardy, L. Wang, P. Burger, T. Wolf, P. Schweiss, and C. Meingast, arXiv:1412.7038

[20] S. Ducatman, N. B. Perkins, and A. V. Chubukov, Phys. Rev. Lett. **109**, 157206, (2012); S. Ducatman, R. M. Fernandes, and N. B. Perkins, Phys. Rev. B **90**, 165123 (2014).

[21] In principle, the system may develop incommensurate magnetic order before the transition ecomes first-order [4]. We do not consider this possibility as experiments on hole-doped $Ba_{1-x}K_xFe_2As_2$ indicate that the SDW transition is first-order.

[22] X. Wang and R. M. Fernandes, Phys. Rev. B **89**, 144502 (2014)

[23] E. Berg, S. A. Kivelson, and D. J. Scalapino, Phys. Rev. B **81**, 172504 (2010).

[24] G. Giovannetti, C. Ortix, M. Marsman, M. Capone, J. van den Brink, and J. Lorenzana, Nature Comm. **2**, 398 (2011).

[25] X. Wang, J. Kang, and R. M. Fernandes, arXiv:1410.6789

[26] S. Maiti, M. M. Korshunov, T. A. Maier, P. J. Hirschfeld, and A. V. Chubukov, Phys. Rev. B **84**, 224505 (2011); *ibid* Phys. Rev. Lett. **107**, 147002 (2011).

[27] F. Kretzschmar, B. Muschler, T. Böhm, A. Baum, R. Hackl, H.-H. Wen, V. Tsurkan, J. Deisenhofer, and A. Loidl, Phys. Rev. Lett. **110**, 187002 (2013).

[28] T. Böhm, A. F. Kemper, B. Moritz, F. Kretzschmar, B. Muschler, H.-M. Eiter, R. Hackl, T. P. Devereaux, D. J. Scalapino, and Hai-Hu Wen, arXiv:1409.6815

[29] J. Kang, A. F. Kemper, and R. M. Fernandes, Phys. Rev. Lett. **113**, 217001 (2014)

[30] R. M. Fernandes, D. K. Pratt, W. Tian, J. Zarestky, A. Kreyssig, S. Nandi, M. G. Kim, A. Thaler, N. Ni, P. C. Canfield, R. J. McQueeney, J. Schmalian, and A. I. Goldman, Phys. Rev. B **81**, 140501 (2010).

[31] E. Wiesenmayer, H. Luetkens, G. Pascua, R. Khasanov, A. Amato, H. Potts, B. Banusch, H.-H. Klauss, and D. Johrendt, Phys. Rev. Lett. **107**, 237001 (2011).

[32] M. Yi, Y. Zhang, Z.-K. Liu, X. Ding, J.-H. Chu, A. F. Kemper, N. Plonka, B. Moritz, M. Hashimoto, S.-K. Mo, Z. Hussain, T. P. Devereaux, I. R. Fisher, H. H. Wen, Z.-X. Shen, and D. H. Lu, Nature Comm. **5**, 3711 (2014).

[33] K. Kuroki, H. Usui, S. Onari, R. Arita, and H. Aoki, Phys. Rev. B **79**, 224511 (2009).

[34] S. Graser, T. A. Maier, P. J. Hirschfeld, and D. J. Scalapino, New J. Phys. **11**, 025016 (2009).

[35] C. Platt, R. Thomale, C. Honerkamp, S.-C. Zhang, and W. Hanke, Phys. Rev. B **85**, 180502(R) (2012).

[36] W.-G. Yin, C.-C. Lee, and W. Ku, Phys. Rev. Lett. **105**, 107004 (2010).

Supplementary for "Interplay between tetragonal magnetic order, stripe magnetism, and superconductivity in iron-based materials"

I. DERIVATION OF THE FREE-ENERGY IN THE ABSENCE OF SUPERCONDUCTIVITY

We first discuss the free-energy of the pure magnetic system, which is given, up to sixth-order in the magnetic order parameters, by:

$$\begin{aligned} F(\boldsymbol{M}_i) =& \frac{a}{2}\left(\boldsymbol{M}_1^2+\boldsymbol{M}_2^2\right)+\frac{u}{4}\left(\boldsymbol{M}_1^2+\boldsymbol{M}_2^2\right)^2-\frac{g}{4}\left(\boldsymbol{M}_1^2-\boldsymbol{M}_2^2\right)^2+w\left(\boldsymbol{M}_1\cdot\boldsymbol{M}_2\right)^2 \\ &-\frac{v}{6}\left(\boldsymbol{M}_1^2-\boldsymbol{M}_2^2\right)^2\left(\boldsymbol{M}_1^2+\boldsymbol{M}_2^2\right)+\frac{\gamma}{6}\left(\boldsymbol{M}_1^2+\boldsymbol{M}_2^2\right)^3+\frac{\lambda}{6}\left(\boldsymbol{M}_1\cdot\boldsymbol{M}_2\right)^2\left(\boldsymbol{M}_1^2+\boldsymbol{M}_2^2\right) \end{aligned} \tag{S1}$$

To calculate the coefficients in Eqn. (S1), we follow Ref. [S1] and start from the Hamiltonian $H = H_0 + H_{\rm int}$, where H_0 is the 3-band non-interacting Hamiltonian discussed in Eq. (1) of the main text, and $H_{\rm int}$ contains the projections of all interactions into the SDW channel. We decouple these interaction terms by Hubbard-Stratonovich transformations and introduce the fields $\boldsymbol{M}_i(\boldsymbol{q}) = U_{SDW}\sum_k c^\dagger_{\boldsymbol{k}+\boldsymbol{q},h}\frac{\boldsymbol{\sigma}}{2}c_{\boldsymbol{k}+\boldsymbol{Q}_i,e_i}$, whose mean values are the magnetic order parameters. The interacting Hamiltonian becomes:

$$H_{SDW} = \sum_{\mathbf{k},i}\left[\boldsymbol{M}_i\cdot\left(c^\dagger_{\boldsymbol{k}+\boldsymbol{q},h}\frac{\boldsymbol{\sigma}}{2}c_{\boldsymbol{k}+\boldsymbol{Q}_i,e_i}+\text{h.c.}\right)+\frac{\boldsymbol{M}_i^2}{2U_{SDW}}\right] \tag{S2}$$

To simplify the notation, it is convenient to write H_0 and H_{SDW} in the basis of a Nambu spinor ψ,

$$H_{SDW} = \sum_{\mathbf{k}}\psi^\dagger_{\mathbf{k}}\hat{H}_{1,\mathbf{k}}(\boldsymbol{M}_i)\psi_{\mathbf{k}} \qquad H_0 = \sum_{\mathbf{k}}\psi^\dagger_{\mathbf{k}}\hat{H}_0\psi_{\mathbf{k}}\ . \tag{S3}$$

Because the Hamiltonian is now quadratic in the fermions, they can be integrated out in the partition function, and the partition function can be expressed as the functional integral over $\mathbf{M}_i$ fields

$$\begin{aligned} Z &\propto \int \mathcal{D}\boldsymbol{M}_i \det\left(\hat{G}_0^{-1}-\hat{G}_1\right)\exp\left(-\int\left(\frac{\boldsymbol{M}_1^2+\boldsymbol{M}_2^2}{2U_{SDW}}\right)\right) \\ &= \det(\hat{G}_0^{-1})\int \mathcal{D}\boldsymbol{M}_i \det\left(1-\hat{G}_0\hat{H}_1\right)\exp\left(-\int\left(\frac{\boldsymbol{M}_1^2+\boldsymbol{M}_2^2}{2U_{SDW}}\right)\right) \end{aligned} \tag{S4}$$

Here $\hat{G}_0$ is the Green's function of the free fermions, $\hat{G}_0 = i\omega_n\hat{I}-\hat{H}_0$. Expanding the action in powers of the order parameters $\boldsymbol{M}_i$ we obtain

$$Z = \int \mathcal{D}\boldsymbol{M}_i \exp(-S_{eff}) \tag{S5}$$

$$\begin{aligned} S_{eff} &= -\ln\det(1-\hat{G}_0\hat{H}_1)+\frac{\boldsymbol{M}_1^2+\boldsymbol{M}_2^2}{2U_{SDW}} \\ &= -\text{tr}\ln(1-\hat{G}_0\hat{H}_1)+\frac{\boldsymbol{M}_1^2+\boldsymbol{M}_2^2}{2U_{SDW}} = \sum_n\frac{1}{n}\text{tr}\left(\hat{G}_0\hat{H}_1\right)^n+\frac{\boldsymbol{M}_1^2+\boldsymbol{M}_2^2}{2U_{SDW}} \end{aligned} \tag{S6}$$

It is now straightforward to derive the coefficients of Eq. (S1). For the quartic coefficients, we find $w = 0$ and:

$$\begin{aligned} &u = A+B\ , \quad g = B-A \\ &A = \int_k \left(G_h(\mathbf{k})\right)^2\left(G_{e_1}(\mathbf{k}+\boldsymbol{Q}_1)\right)^2 = \int_k\left(\frac{1}{i\omega+\epsilon}\right)^2\left(\frac{1}{i\omega-\epsilon-\delta_\mu-\delta_m\cos 2\theta}\right)^2\ , \\ &B = \int_k \left(G_h(\mathbf{k})\right)^2 G_{e_1}(\mathbf{k}+\boldsymbol{Q}_1)G_{e_2}(\mathbf{k}+\boldsymbol{Q}_2) = \int_k\left(\frac{1}{i\omega+\epsilon}\right)^2\frac{1}{i\omega-\epsilon-\delta_\mu-\delta_m\cos 2\theta}\frac{1}{i\omega-\epsilon-\delta_\mu+\delta_m\cos 2\theta}\ . \end{aligned} \tag{S7}$$

Here, $G_a(\boldsymbol{k})$ is the free-fermion Green's function for pocket a, $G_a^{-1}(\mathbf{k}) = i\omega_n - \epsilon_a(\mathbf{k})$, and $\int_k \to T\sum_n \int \frac{\mathrm{d}^d k}{(2\pi)^d}$, with Matsubara frequency $\omega_n = (2n+1)\pi T$. After integrating over the momentum we obtain:

$$\begin{aligned} A =& N_f T\pi \sum_{n=0}^{\infty} \Im \int_\theta \frac{1}{\left(i\omega_n + \frac{\delta_\mu}{2} + \frac{\delta_m}{2}\cos 2\theta\right)^3} \\ B =& N_f T\pi \sum_{n=0}^{\infty} \Im \int_\theta \frac{i\omega_n + \frac{\delta_\mu}{2}}{\left(\left(i\omega_n + \frac{\delta_\mu}{2}\right)^2 - \left(\frac{\delta_m}{2}\cos 2\theta\right)^2\right)^2} \end{aligned} \tag{S8}$$

with $\int_\theta = \int \frac{\mathrm{d}\theta}{2\pi}$ and N_f is the density of states. For the sixth-order coefficients, we obtain $\lambda = 0$ and:

$$\begin{aligned} &\gamma = C + 3D\ , \qquad v = 3(D-C) \\ C =& \int_k \left(G_h(\mathbf{k})\right)^3 \left(G_{e_1}(\mathbf{k}+\boldsymbol{Q}_1)\right)^3 = N_f T\pi \frac{3}{4} \sum_{n=0}^{\infty} \Im \int_\theta \frac{1}{\left(i\omega_n + \frac{\delta_\mu}{2} + \frac{\delta_m}{2}\cos 2\theta\right)^5} \quad , \\ D =& \int_k \left(G_h(\mathbf{k})\right)^3 \left(G_{e_1}(\mathbf{k}+\boldsymbol{Q}_1)\right)^2 G_{e_2}(\mathbf{k}+\boldsymbol{Q}_2) \\ =& \frac{N_f T\pi}{8} \sum_{n=0}^{\infty} \Im \int_\theta \frac{3}{\left(i\omega_n + \frac{\delta_\mu}{2} + \frac{\delta_m}{2}\cos 2\theta\right)^4 \left(i\omega_n + \frac{\delta_\mu}{2} - \frac{\delta_m}{2}\cos 2\theta\right)} \\ &+ \frac{2}{\left(i\omega_n + \frac{\delta_\mu}{2} + \frac{\delta_m}{2}\cos 2\theta\right)^3 \left(i\omega_n + \frac{\delta_\mu}{2} - \frac{\delta_m}{2}\cos 2\theta\right)^2} \\ &+ \frac{1}{\left(i\omega_n + \frac{\delta_\mu}{2} + \frac{\delta_m}{2}\cos 2\theta\right)^2 \left(i\omega_n + \frac{\delta_\mu}{2} - \frac{\delta_m}{2}\cos 2\theta\right)^3} \ . \end{aligned} \tag{S9}$$

We can now evaluate g numerically at any temperature and analytically at high temperatures and at $T = 0$. For $T \gg \delta_\mu$ and $T \gg \delta_m$ we obtain:

$$\begin{aligned} A \approx& N_f T\pi \Im \int_\theta \sum_{n=0}^{\infty} \frac{1}{(i\omega_n)^3} \left(1 - 3\frac{\delta_\mu + \delta_m \cos 2\theta}{2i\omega_n} + 6\left(\frac{\delta_\mu + \delta_m \cos 2\theta}{2i\omega_n}\right)^2\right) \\ B \approx& N_f T\pi \Im \int_\theta \sum_{n=0}^{\infty} \frac{1}{(i\omega_n)^3} \left(1 - 3\frac{\delta_\mu}{2i\omega_n} + 2\left(\frac{\delta_m \cos 2\theta}{2i\omega_n}\right)^2 + 6\left(\frac{\delta_\mu}{2i\omega_n}\right)^2\right) \\ g =& B - A \approx -N_f T\pi \Im \int_\theta \sum_{n=0}^{\infty} \frac{(\delta_m \cos 2\theta)^2}{(i\omega_n)^5} = \frac{\pi T N_f \delta_m^2}{2(2\pi T)^5} \sum_{n=0}^{\infty} \frac{1}{(n+1/2)^5} = \frac{31\zeta(5) N_f \delta_m^2}{64\pi^4 T^4} \ . \end{aligned} \tag{S10}$$

At $T = 0$ we have $T\sum_n \to \int \frac{\mathrm{d}\omega}{2\pi}$. To regularize the integral, we add the lifetime $\mathrm{sign}(\omega_n)/(2\tau)$ to the fermion propagator and take the limit $\tau \to \infty$ after we compute g. We obtain:

$$\begin{aligned} A =& -N_f \int_\theta \Re \left(\frac{1}{\delta_\mu + \delta_m \cos 2\theta + i/\tau}\right)^2 \\ B =& -N_f \int_\theta \Re \frac{1}{(\delta_\mu + \delta_m \cos 2\theta + i/\tau)(\delta_\mu - \delta_m \cos 2\theta + i/\tau)} \end{aligned} \tag{S11}$$

$$g = B - A = \frac{N_f}{2} \int_\theta \Re \left(\frac{1}{\delta_\mu + \delta_m \cos 2\theta + i/\tau} - \frac{1}{\delta_\mu - \delta_m \cos 2\theta + i/\tau}\right)^2 \tag{S12}$$

At $T_N \to 0$, $|\delta_\mu| > \delta_m$ (see Ref. [S2]). In this case we can safely set $\tau = \infty$ in the integrals in (S12) and obtain:

$$g = \frac{\delta_m^2 N_f}{|\delta_\mu|(\delta_\mu^2 - \delta_m^2)^{3/2}} \geq 0 \ . \tag{S13}$$

If this condition was not satisfied, i.e. if $|\delta_\mu| \leq \delta_m$, τ^{-1} must remain finite to avoid a divergence in g. Analytical evaluation of the integral then reveals that $g \propto 1/\tau$ and

$$g > 0 \text{ if } |\delta_\mu| < \delta_m/2 \ . \tag{S14}$$

For intermediate temperatures we evaluate g – and also v – numerically. The result is shown in Fig. S1 in the $\delta_\mu/(2\pi T)$, $\delta_m/(2\pi T)$ plane. We see that, as temperature decreases and one tracks the magnetic transition line $T_N(x)$, there is a sequence of changes from $g > 0$ to $g < 0$ and then back to $g > 0$ (the arrow in the plot represents a schematic path along the magnetic transition line). In Fig. 1 in the main text, we plotted a cut for the fixed value $\delta_m/(2\pi T) = 1$, which is representative of this behavior. We plot again this cut in Fig. S1, together with the behavior of u and γ. As discussed in the main text, there is a regime inside the C_4 phase where $u < 0$ and $\gamma > 0$, which implies that the SDW transition is first order.

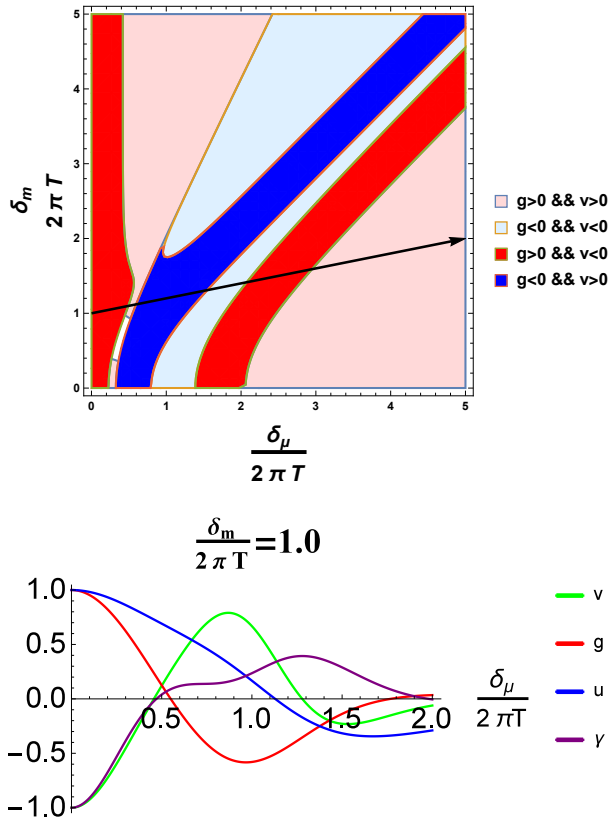

FIG. S1: (**upper panel**) The signs of g and v as a function of $\delta_\mu/(2\pi T)$ and $\delta_m/(2\pi T)$. The arrow represents schematically a path along the magnetic transition line $T = T_N(x)$, in which δ_m is a constant and δ_μ increases with doping. The arrow points towards larger doping. (**lower panel**) The quartic (u, g) and sixth-order (v, γ) SDW coefficients as a function of $\delta_\mu/(2\pi T)$ when $\delta_m/(2\pi T)$ is fixed to be 1.0. Note that these coefficients are normalized by their values at $\delta_\mu = 0$.

II. DERIVATION OF THE FREE ENERGY IN THE PRESENCE OF SUPERCONDUCTIVITY

The free-energy in the presence of both SC and SDW degrees of freedom is given by:

$$\begin{aligned} F(\boldsymbol{M}_i, \Delta_m) =& F(\boldsymbol{M}_i) + \frac{\alpha_s}{2}|\Delta_{s\pm}|^2 + \frac{\alpha_d}{2}|\Delta_d|^2 + \frac{\beta_s}{4}|\Delta_{s\pm}|^4 + \frac{\beta_d}{4}|\Delta_d|^4 \\ &+ c_s|\Delta_{s\pm}|^2\left(\boldsymbol{M}_1^2 + \boldsymbol{M}_2^2\right) + c_d|\Delta_d|^2\left(\boldsymbol{M}_1^2 + \boldsymbol{M}_2^2\right) + c_{sd}\left(\Delta_{s\pm}^*\Delta_d + \text{h.c.}\right)\left(\boldsymbol{M}_1^2 - \boldsymbol{M}_2^2\right) \end{aligned} \tag{S15}$$

To derive the SC coefficients, we need to account also for the interactions in $H_{\rm int}$ that promote superconductivity. Following Ref. [S3], we express them in terms of the inter-band pairing interactions $U_{eh} > 0$ (between the hole pocket and either of the electron pockets) and $U_{ee} > 0$ (between the two electron pockets). Introducing the gap function at each pocket, $\Delta_i = \sum_{\boldsymbol{k},j} U_{ij} c_{-\boldsymbol{k},j\downarrow} c_{\boldsymbol{k},j\uparrow}$, we write the interacting SC Hamiltonian as

$$H_{SC} = \sum_{\boldsymbol{k},ij} \left[\left(\Delta_i c^\dagger_{\boldsymbol{k},i\uparrow} c^\dagger_{-\boldsymbol{k},i\downarrow} + \text{h.c.} \right) \delta_{ij} + \frac{1}{2} \Delta_i U^{-1}_{ij} \Delta^*_j \right] \tag{S16}$$

To proceed, we repeat the same steps as in the previous section, but with $H_{SDW} + H_{SC}$ instead of H_{SDW}. It is convenient to switch to a parametrization of the superconducting order parameters in terms of the irreducible representations A_{1g} ($s_\pm$ and s_{++} states) and B_{1g} (d-wave state) [S3]:

$$\begin{pmatrix} \Delta_h \\ \Delta_{e_1} \\ \Delta_{e_2} \end{pmatrix} = \begin{pmatrix} \sin\phi & -\cos\phi & 0 \\ \frac{\cos\phi}{\sqrt{2}} & \frac{\sin\phi}{\sqrt{2}} & -\frac{1}{\sqrt{2}} \\ \frac{\cos\phi}{\sqrt{2}} & \frac{\sin\phi}{\sqrt{2}} & \frac{1}{\sqrt{2}} \end{pmatrix} \begin{pmatrix} \Delta_{s_{++}} \\ \Delta_{s_\pm} \\ \Delta_d \end{pmatrix} \tag{S17}$$

where the parameter ϕ depends on the ratio of the pairing interactions:

$$\tan\phi = \frac{\sqrt{8U^2_{eh} + U^2_{ee}} - U_{ee}}{2\sqrt{2} U_{eh}} \tag{S18}$$

Note that the SC gaps in the $s_\pm$ state have different signs in the hole and electron pockets:

$$\Delta_{e_1} = \Delta_{e_2} = -\frac{\tan\phi}{\sqrt{2}} \Delta_h \ . \tag{S19}$$

In the s_{++} state, on the other hand, all SC gaps have the same sign:

$$\Delta_{e_1} = \Delta_{e_2} = \frac{\cot\phi}{\sqrt{2}} \Delta_h \ . \tag{S20}$$

In the d-wave state, the gap in the hole pocket averages to 0 and the gaps in the two electron pockets have opposite signs.

Applying this transformation and ignoring the $\Delta_{s_{++}}$ contributions we obtain:

$$\begin{aligned} F(\boldsymbol{M}_i, \Delta_m) = F(\boldsymbol{M}_i) &+ \frac{1}{2} \left(a_{sh} \cos^2\phi + a_{se} \sin^2\phi \right) |\Delta_{s_{+-}}|^2 + \frac{1}{2} a_{se} |\Delta_d|^2 \\ &+ \frac{1}{4} \left(u_{sh} \cos^4\phi + \frac{1}{2} u_{se} \sin^4\phi \right) |\Delta_{s_{+-}}|^4 + \frac{1}{8} u_{se} |\Delta_d|^4 + \frac{1}{4} u_{se} \sin^2\phi |\Delta_{s_{+-}}|^2 |\Delta_d|^2 \left(1 + 2\cos^2\theta \right) \\ &+ \left[\frac{1}{2} \left(\gamma_h \cos^2\phi + \frac{1}{2} \gamma_e \sin^2\phi - \frac{1}{\sqrt{2}} \gamma_{he} \sin 2\phi \right) |\Delta_{s_{+-}}|^2 + \frac{1}{4} \gamma_e |\Delta_d|^2 \right] \left(\boldsymbol{M}_1^2 + \boldsymbol{M}_2^2 \right) \\ &+ \frac{1}{2} \left(\frac{1}{\sqrt{2}} \gamma_{he} \cos\phi - \frac{1}{2} \gamma_e \sin\phi \right) \left(\Delta^*_{s\pm} \Delta_d + \Delta_{s\pm} \Delta^*_d \right) \left(\boldsymbol{M}_1^2 - \boldsymbol{M}_2^2 \right) \end{aligned} \tag{S21}$$

The coupling constants describing the interplay between SC and SDW are given by:

$$\begin{aligned} \gamma_h &= 16 \sum_k G^2_{hk} \tilde{G}_{hk} G_{e_1 k} \\ \gamma_e &= 16 \sum_k G^2_{e_1 k} \tilde{G}_{e_1 k} G_{hk} \\ \gamma_{he} &= 8 \sum_k G_{hk} \tilde{G}_{hk} G_{e_1 k} \tilde{G}_{e_1 k} \end{aligned} \tag{S22}$$

Here $\tilde{G}$ is the Green function for the hole states, $\tilde{G} = (-G)^*$. The coefficients of Eq. (S15) are given by:

$$\begin{aligned} c_s &= \frac{1}{2} \left(\gamma_h \cos^2\phi + \frac{1}{2} \gamma_e \sin^2\phi - \frac{1}{\sqrt{2}} \gamma_{he} \sin 2\phi \right) \\ c_d &= \frac{1}{4} \gamma_e \\ c_{sd} &= \frac{1}{2} \left(\frac{1}{\sqrt{2}} \gamma_{he} \cos\phi - \frac{1}{2} \gamma_e \sin\phi \right) \end{aligned} \tag{S23}$$

At perfect nesting, where $\delta_\mu = \delta_2 = 0$, we find that $\gamma_h = \gamma_e = 2\gamma_{he} = \frac{14\zeta(3)N_F}{\pi^2 T^2}$. In the limit where $U_{he} \gg U_{ee}$, $\phi \to \pi/4$ and we find that $c_s = \left(3-\sqrt{2}\right)\gamma_h/8 > 0$. The positive sign of c_s is evidence of the competition between $s_\pm$ SC and SDW. Of course, the value of c_s depends on the parameter ϕ, which is sensitive to the ratio between the pairing interactions U_{he} and U_{ee}. In particular, for $U_{he} > U_{ee}$, the ground state is $s_\pm$ whereas for $U_{he} < U_{ee}$, the ground state is d-wave. Thus, to describe the $Ba_{1-x}K_xFe_2As_2$ system, for which the $s_\pm$ and d-wave states are close in energy, we take U_{ee} to be somewhat below U_{he}. For practical calculations, we used $U_{ee} = U_{he}/2$. In Fig S2 we show the behavior of the coupling constants c_i as functions of $\delta_\mu/(2\pi T)$ for a fixed $\delta_m/(2\pi T) = 1$. The coupling c_s is positive in a wide doping range and, in particular, in almost the entire doping range where the C_4 phase exists (see Fig. S1) and where the T_c transition line crosses the T_N transition line, according to the experiments in $Ba_{1-x}K_xFe_2As_2$.

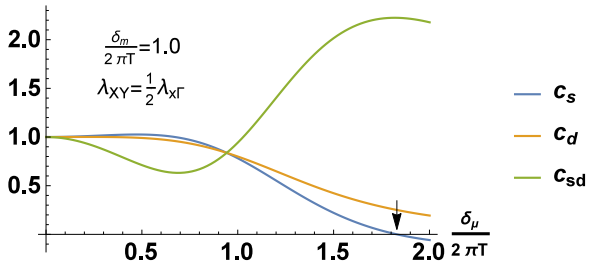

FIG. S2: Coupling constants c_s, c_d, and c_{sd}, describing the interplay between the SDW and SC order parameters, as function of $\delta_\mu/(2\pi T)$ for a fixed $\delta_m/(2\pi T) = 1$. The couplings constants are normalized to their values at zero doping ($\delta_\mu = 0$). The arrow shows the value where c_s changes sign, which according to Fig. S1 happens very close to the $C_4 \to C_2$ transition point.

[S1] R. M. Fernandes, A. V. Chubukov, J. Knolle, I. Eremin and J. Schmalian, Phys. Rev. B **85**, 024534 (2012).
[S2] A. B. Vorontsov, M. G. Vavilov, and A. V. Chubukov, Phys. Rev. B **81**, 174538 (2010).
[S3] R. M. Fernandes and A. J. Millis, Phys. Rev. Lett. **111**, 127001 (2013).